Hydroquinone Synthesis of Silver Nanoparticles: A Simple Model Reaction To Understand the Factors That Determine Their Nucleation and Growth

ARTICLE *in* CRYSTAL GROWTH & DESIGN · FEBRUARY 2008

Impact Factor: 4.89 · DOI: 10.1021/cg7009644

4 AUTHORS, INCLUDING:

Manuel Alejo Perez
National University of Cordoba, Argentina
23 PUBLICATIONS **229** CITATIONS
SEE PROFILE

Raquel Moiraghi
National University of Cordoba, Argentina
6 PUBLICATIONS **50** CITATIONS
SEE PROFILE

Eduardo Andres Coronado
National University of Cordoba, Argentina
60 PUBLICATIONS **5,324** CITATIONS
SEE PROFILE

CRYSTAL GROWTH & DESIGN
2008
VOL. 8, NO. 4
1377–1383

Hydroquinone Synthesis of Silver Nanoparticles: A Simple Model Reaction To Understand the Factors That Determine Their Nucleation and Growth

M. A. Pérez,* R. Moiraghi, E. A. Coronado, and V. A. Macagno

INFIQC - Departamento de Fisicoquímica, Facultad de Ciencias Químicas, Universidad Nacional de Córdoba, Ciudad Universitaria, 5000 Córdoba, Argentina

Received October 4, 2007; Revised Manuscript Received December 20, 2007

ABSTRACT: A simple experimental model system based on the reaction between silver(I) and a hydroquinone has been used to investigate the synthesis of silver nanoparticles (NPs) in aqueous media. Progressive nucleation and autocatalytic surface growth were found to be the relevant processes that control the morphology. The effect of synthetic parameters (such as the chemical nature of the metallic precursor, hydroquinone concentration, stabilization agents, and ligands) on the NP nucleation and growth are discussed on the basis of the optical properties, morphological characterization, and electrodynamics calculations. A very important dependence of the final morphology of the NPs on the procedure of mixing of reactants was found to be connected to the nature of the metallic precursor. Ammonia solutions containing strong stabilization agents were demonstrated to help to control shape and size by quenching autocatalytic surface growth.

Introduction

Metal nanoparticles have a number of properties that could be tuned or enhanced through the nanoscale control of morphology. It is now well established that on the nanometer scale, the chemical, electrical, mechanical, and optical properties of nanoparticles can be altered just by changing their size and morphology.[1] In the particular case of noble metal nanoparticles (NPs) such as silver and gold, it has been demonstrated, for example, that they are able to amplify the local electric field many orders of magnitude, an effect responsible for the enhancement of Raman signals by a factor of 10^4-10^6, reaching in some cases the single molecule level.[2] These properties could be useful for the design of chemical sensors, optical twisters, optical filters, etc.[3] Given the range of applications in which noble metal NPs are important, better control of their properties is critical, and it can only be achieved by a better control of their size and morphology.

It has been argued that this control over the size and shape of NPs can be attained by the separation of nucleation and growth stages. One approach is to enable the nucleation and growth of NPs to take place in separate time frames by a programmed temperature control as, for example, in the hot-injection method.[4] This one-pot synthetic method has been successfully used to produce metal and semiconductor NPs with remarkable small size dispersion ($\leq 10\%$). Some disadvantages can be mentioned, however, such as the need to drive the reaction at high temperatures in high-boiling nonpolar coordinating solvent (trioctylphosphineoxide), as well as the use of organometallic compounds as precursor agents. A second alternative is to physically separate nucleation from growth by changing the chemical conditions to drive each stage separately. This is the main strategy used in the production of nonspherical gold NPs in aqueous solutions, the so-called seed-mediated growth method.[5–8] Nucleation is driven, in a first step, with the help of a strong reducing agent (sodium borohydride) to produce gold seeds (mainly spherical NPs with diameter smaller than 5 nm) in an aqueous solution containing the metallic precursor agent ($HAuCl_4$). Subsequently, these seeds are added into an amplification bath (where no further nucleation can occur) to drive the growth of these small particles into larger gold nanorods[6–9] and nanodiamonds.[7] Although this method allows production of NPs with shapes different from the sphere, the mechanisms controlling the anisotropic growth are not well understood.[10,11] As a consequence, the discussion about the reproducibility of the experiments that produces NPs of a given size and shape is a matter that has just recently been the focus of research.[10]

The control over shape and size for silver NPs seems to be more difficult than that for gold, even under similar conditions.[12] The seed-mediated method has been used for the production of silver nanorods[13] and plated NPs.[14,15] In all these studies the capping action of cetyltrimethylammonium bromide (CTAB) has been considered to be crucial for the anisotropic growth of nanorods; however, some recent work should be noted where that hypothetic capping action of CTAB has been questioned.[15]

Besides the valuable contribution of these studies within the synthetic field, a deeper insight to envisage the mechanisms underneath is needed. Because the synthesis and formation of metal NPs involves a complex sequence of events such as mixing of the reactants, reduction of the metallic precursor, nucleation, growth, and stabilization, the first question that arises is what should be the experimental system of choice, given the difficulties mentioned above. Such a system should be simple enough to get a clear understanding of the influence of each synthetic variable on the final NP morphology. Regarding the metallic precursor, silver is a better candidate than gold because the relevant silver electrochemistry lies on a single-electron process. Following this criterion of simplicity, the use of reducing agents involving complex multielectronic processes that are frequently not well characterized, such as citrate, BH_4^-, or ascorbate, should be avoided. These reducing agents also generate oxidation and decarboxylation products that could act as adsorbates as well.[16] In contrast, hydroquinone (H_2Q) exhibits a simple redox reaction[17] the two-electron oxidation of which to yield the quinone and protons takes place with no remarkable changes in the molecular structure. In addition, the fact that hydroxyl (—OH) and ketone (═O) are uncharged functional

* Corresponding author. Fax+54 351 4334188. E-mail address: mperez@fcq.unc.edu.ar.

10.1021/cg7009644 CCC: $40.75
Published on Web 02/22/2008

groups renders a capping action of either of the couple species unlikely. Thus, the reaction between the silver ion and hydroquinone constitutes a suitable and simple experimental model system to investigate the effect of different synthetic conditions on the morphology of the NPs. Such a model system together with an adequate choice of coreactants would improve the understanding of the role played separately by each component of the reactive solution.[16]

In this paper, we examine the nucleation and growth of silver NPs in aqueous solution on the basis of the reaction of the silver ion precursor and hydroquinone as the reducing agent. This reaction is slow enough to allow us to make a careful analysis of the processes mentioned above. The evolution of the optical properties of the NPs is used to monitor the changes in their size and shape with the aid of electrodynamics calculations. The final morphology of the NPs is characterized with transmission electron microscopy (TEM) and contrasted with their optical behavior. The effect of the nature of the metallic precursor, the concentration of the reducing agent, the concentration and chemical nature of the capping agents, and pH has been studied. We have also analyzed the effect of mixing of reactants, this aspect being so critical that it could determine the final morphology of the NPs. For this reason, most of the present work is focused on how the effect of mixing can be minimized.

Experimental Section

Synthesis. All aqueous solutions were prepared from AR chemicals and purified water (Milli Ro, Milli Q system). In a typical synthesis, silver nanoparticles are grown at room temperature (25 °C) by the mixing of solutions containing $AgNO_3$ (precursor) and hydroquinone (H_2Q) (reducing agent) to obtain 15 mL of the reactive solution. All concentration values reported for the reactive solution correspond to the nominal values calculated from the concentration values of the stock solutions and considering the dilution of each aliquot after the mixing of the reactants species. For the reactive solution, $AgNO_3$ concentration was fixed at 100 μM, whereas H_2Q concentration was varied from 5 to 50 μM. Additional compounds (coreactants), such as tetramethylammonium hydroxide ($N(CH_3)_4OH$), herein referred to as TMA(OH), ammonia (NH_3), and ammonium chloride (NH_4Cl), were also used to study the growth of NPs under controlled pH and the action of different stabilization agents, and their respective concentrations are provided when necessary. In order to prevent inaccuracy in the hydroquinone concentration due to the oxidation by atmospheric oxygen, only 2000 μM H_2Q stock solutions freshly prepared were used. The mixing of the metallic precursor and the reducing agent to obtain the reactive solution was performed according to following procedures.

Protocol 1 (**P1**).A volume V_a (usually $\leq$100 μL) of the H_2Q stock solution (2000 μM) is added directly to 15 mL of 100 μM $AgNO_3$ (and coreactants) solution and quickly homogenized. Note that the addition of V_a to 15 mL produces a negligible volume change. Concentration of reducing agents before mixing is 400-fold their respective value in the reactive solution.

Protocol 2 (**P2**).A volume V_a ($\leq$100 μL) of the H_2Q stock solution is diluted with water up to 7.5 mL and mixed subsequently with 7.5 mL of a 200 μM $AgNO_3$ solution and quickly homogenized to give 15 mL of the reactive solution. Concentrations of the metallic precursor and the reducing agents before the mixing are just 2-fold their respective value in the reactive solution. When coreactants were used, their concentration was the same in both aliquots.

In order to reach a better appreciation of the influence of the different factors (concentration, chemical nature of metallic precursors, coreactants, etc.), we found it convenient to focus the analysis mainly on the experiments performed with a silver content (100 μM $AgNO_3$) much higher than that of hydroquinone (5 μM H_2Q); further arguments to support this will be provided below. Therefore this combination of concentration values will be referred hereafter as "reactive solution", and the discussion of the effect of H_2Q concentration is left for the end of the final section.

Characterization of NPs. It is well-known that when metal NPs are illuminated they exhibit collective excitation of conduction-band electrons called surface plasmon resonances (SPRs). These SPRs are very sensitive to NP shape and size.[18] In this work UV–vis spectroscopy was used in the 200–1100 nm range to characterize the optical behavior of NPs, recording SPR spectra periodically along the time the reaction lasted (from days to months). Spectra of colloidal NPs were measured using a Shimadzu UV-1200 spectrometer with a 1 cm quartz cell at room temperature. The reaction was assumed to be terminated when no significant changes were registered in SPR spectral series. In all cases, otherwise stated, figures show normalized spectra corresponding to the final product obtained under each synthetic condition investigated. Spectral normalization was carried out by assigning a value of one to the extinction intensity of the SPR peak at the shortest wavelength value ($380 \leq \lambda \leq 440$ nm).

The samples used for NP morphological characterization were prepared without postsynthesis purification by seeding many drops of the colloidal solutions onto a Formvar-covered cooper grid and evaporating then in air at room temperature. The samples were studied with transmission electron microscopy (TEM) by using a JEM-JEOL 1120 microscope. For the sake of clarity, the discussion of the morphological features is performed in terms of the characteristic length (d), which corresponds to the diameter for spherical (or, more precisely, nearly spherical) NPs, whereas for pronounced nonspherical particles (mainly prolate-shaped particles), the characteristic length refers to the length along the longest symmetry axis.

Results and Discussion

Effect of the Mixing Protocols. The first step in any NP synthesis is the mixing of reactants. Although the one-pot synthetic scheme is widely used to prepare NPs, the hot-injection method is the only method that has been fully proven to produce NPs with reproducible morphology.[4] Therefore it is of outmost importance to analyze whether some size and shape control can be achieved in aqueous systems with a "one-pot" approach.

Figure 1a shows the SPR spectra in the UV–visible range corresponding to NPs obtained by using the two different mixing protocols **P1** and **P2**, as described in the Experimental Section. Silver NPs grown using **P1** exhibit a single-peak SPR spectrum with a maximum at 420 nm, which may correspond to the dipole SPR of nearly spherical shapes with d ranging from 10 to 30 nm.[18] For longer wavelength values, the extinction decreases gradually defining a long tail within the 450–1100 nm range. This feature could be associated with the optical behavior of a relatively small population of large NPs ($d > 50$ nm), as well as with nonspherical shapes.[18] The use of **P2** leads to a quite different population of NPs as evidenced by the double-peak SPR spectrum. The broad peak at ~860 nm (II) is associated with the dipole SPR of very large NPs, whereas the peak at 396 nm (I) accounts for the contributions of multipole SPRs of large NPs, as well as of the dipole SPR of small, spherical NPs. Peak I is blue-shifted with respect to the characteristic wavelength values ($\lambda > 400$ nm) of the dipole SPR of small spheres, indicating that this peak has a major contribution from high-order multipole SPRs. This interpretation is consistent with exact electrodynamics calculations performed using Mie theory. Figure 2 shows electrodynamics simulations performed for silver spheres of different diameters, in the range 40–220 nm. For spheres of up to 40 nm, only one extinction peak is observed, whereas the contribution of a quadrupole shoulder at wavelengths less than 400 nm becomes important for sphere diameters greater than 60 nm. As the diameter increases more extinction peaks of higher order appear at shorter wavelengths, and the dipole mode experiences a red shift. These simulations should be taken as reference for the interpretation of the spectra in the present work.[18]

Figure 1b shows one field of NPs produced by protocol **P2**. It pictures how extreme the differences can be in the final NP sizes by showing the presence of very large particles (some with

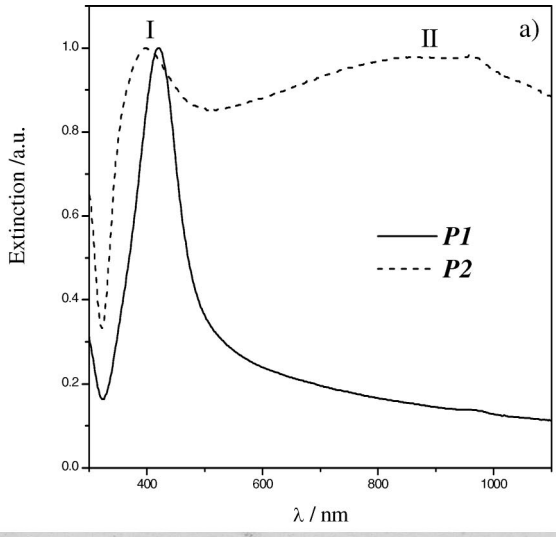

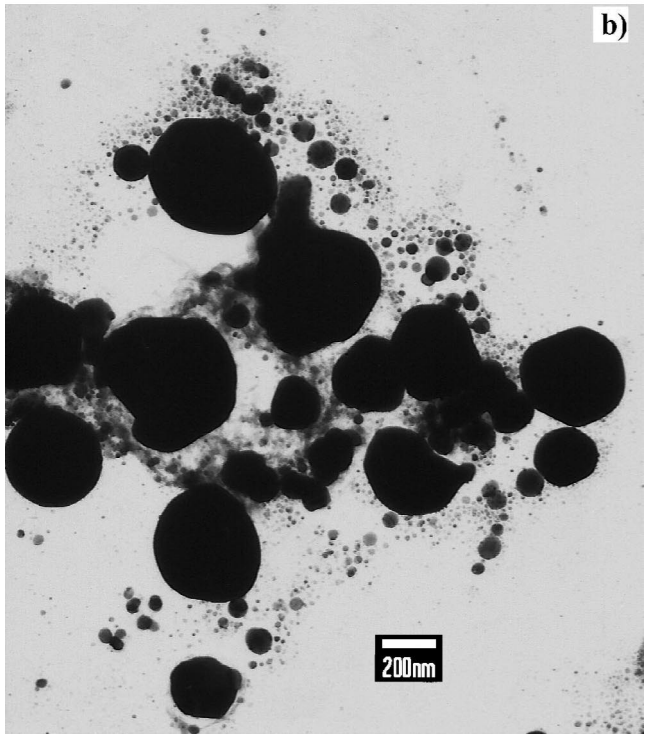

Figure 1. (a) Normalized SPR spectra after 3 months of reaction of NPs prepared under protocol **P1** (—) and **P2** (– – –); (b) TEM image of NPs grown by protocol **P2**. Bar scale = 200 nm. Reactive solution also contains 100 μM TMA(OH).

d > 200 nm), as well as many smaller ones in arrays around the larger ones. The inspection of different fields in the samples show a large number of small NPs, which also might contribute to the extinction spectrum, although their extinction coefficient is smaller than those of the large NPs shown in Figure 1b. It is worth noting that small NPs present variability in the value of d, suggesting the existence of a progressive nucleation taking place simultaneously with the growth process.[19] This issue can be more properly addressed by analyzing the evolution of the SPR spectra during the reaction. Figure 3a,b shows sequences of spectra during the growth of NPs after the mixing performed with protocols **P1** and **P2**, respectively. Arrows in the figure point at the trends observed as the reaction takes place. No remarkable change is observed in the wavelength value for the dipole SPR peak ($420 \leq \lambda \leq 435$ nm) for NPs formed by protocol **P1** (Figure 3a), indicating that small, nearly spherical

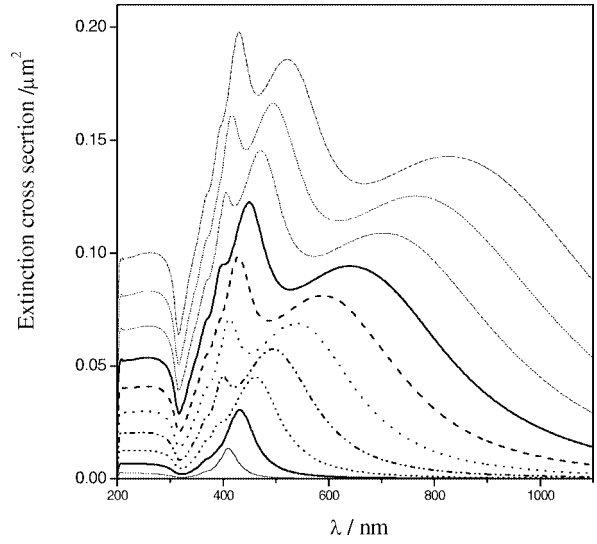

Figure 2. Extinction cross-section vs wavelength for silver spheres of different diameters in water calculated according to Mie's theory. The diameter of the spheres increases from 40 (bottom) to 220 nm (top) in steps of 20 nm.

NPs are the dominant shape that determines the optical behavior during the whole reaction. The peak extinction intensity (at ca. 420 nm) increases constantly with the reaction time indicating that the amount of small spherical particles also increases. The slight increment of peak tail extinction is connected with slow growth of the large NPs. This feature would indicate that with protocol **P1**, progressive nucleation is favored over growth.

For NPs formed by protocol **P2** (Figure 3b), the broad maximum II exhibits a red shift, from 588 to 860 nm, as well as a remarkable broadening during the reaction, indicating that large NPs grow as the reaction time elapses (compare with the simulations in Figure 2). As the reaction occurs, a continuous increase in the extinction of peak I was also observed during the course of the reaction, a further support of the above interpretation. A slight red shift of peak I, from 383 to 397 nm, is also observed. Both trends can be associated with the increase in the contributions of dipole SPR coming from the increasing amount of small, spherical NPs, as well as that of the higher multipole SPRs coming from large NPs, and consequently, a detailed interpretation cannot be obtained. However, the morphological evidence provided supports both the growth of large particles and progressive nucleation (Figure 1b). Although the results for both mixing protocols point to the existence of progressive nucleation, **P2** would favor growth over nucleation, producing large NPs that dominate the optical behavior. These large NPs are easily separated by precipitation; therefore the synthetic scheme using hydroquinone as reducing agent would constitute, within further improvements over the shape and size control, a safer alternative than that based on the reduction with hydrogen gas[21] to produce large NPs with multipole SPRs. The number of peaks in the SPR profiles that characterize the products obtained from each mixing protocol was the same from one experiment to another. The dipole SPR peak wavelength of NPs produced by protocol **P1** showed no remarkable changes among different experiments, although some small differences were observed in the peak tail associated with large NPs. This is an indication that small, nearly spherical NPs can be produced by protocol **P1** with some degree of control.

Even though a progressive nucleation takes place for both mixing protocols, protocols **P1** and **P2** lead to differences in the early stages of reaction. Under isothermal conditions, the

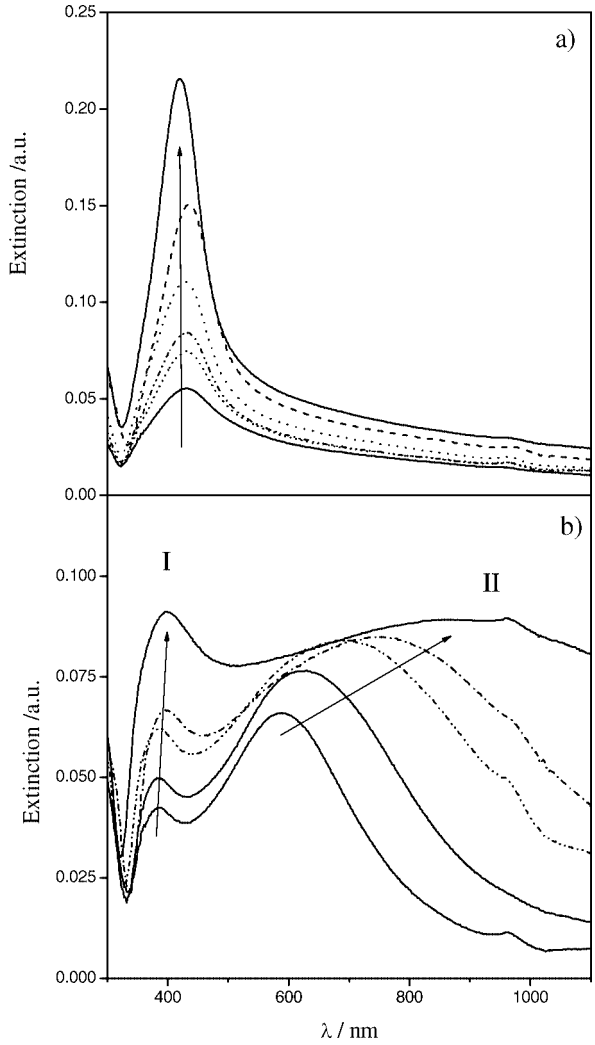

Figure 3. Evolution of the SPR spectra of NPs during the reaction by (a) protocol **P1** and (b) protocol **P2** to obtain a reactive solution also containing 100 μM TMA(OH). Overall reaction time = 3 months.

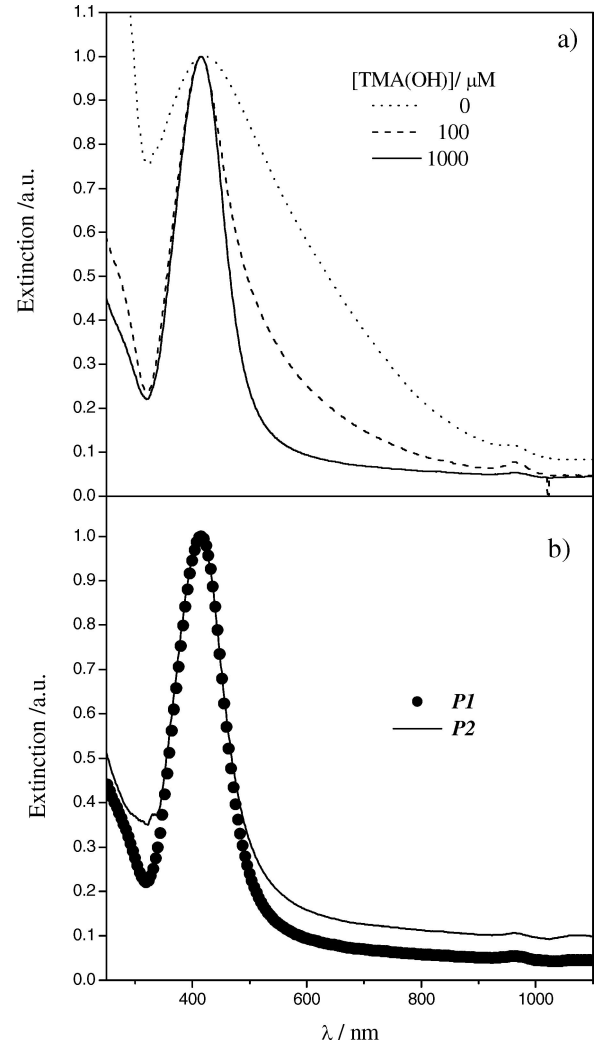

Figure 4. Normalized SPR spectra of NPs prepared in a reactive solution containing 1000 μM NH_3: (a) particles prepared by protocol **P2** for different concentrations of TMA(OH), (---) 0 μM, (———) 100 μM, and (—) 1000 μM; (b) particles prepared by different mixing protocols, (●) **P1** and (—) **P2**, to obtain a reactive solution also containing 1000 μM NH_3 and 1000 μM TMA(OH).

nucleation stage exhibits only dependence on the concentration of reactants; thus the drastic difference between the values for the starting H_2Q concentration before the mixing (2000 μM and 10 μM for **P1** and **P2**, respectively) induces different size and shape distributions. The characteristic dipole SPR peak (430 nm) is observed immediately after the mixing for **P1**, whereas for **P2** a measurable difference in NP extinction is obtained only after a day of reaction (not shown in Figure 3; Figure SA1 in Supporting Information). In summary, the analysis of this section shows that the differences in H_2Q concentration during the early stages of reaction are the crucial factor that determines the morphology of NPs, despite the existence of a progressive nucleation. The present results also stress the importance of the events taking place during the mixing of reactants. In the following sections, we analyze how the control over the shape and size can be improved by quenching the growth stage since a progressive nucleation takes place continuously.

Effect of the Metallic Precursor Nature. The influence of the metallic precursor nature is another factor that should be taken into account in any synthetic strategy if some degree of shape and size control is desired. Our experiments performed in silver ammonia solution indicate that the change of the metallic precursor species can help to improve control over shape and size of NPs. Under conditions where the silver ion is mainly in the form of the complex $[Ag(NH_3)_2]^+$, even the use of protocol **P2** leads to the formation of NPs with single-peak SPR spectra similar to that shown in Figure 1a, indicating that small, nearly spherical particles govern the optical properties. Thus, ammoniacal silver ions would help, in principle, to control the growth of NPs. Taking into account that an autocatalytic surface mechanism has been observed for the growth of cluster catalysts in organic solvents,[19,20] it would seem reasonable to attribute the quenching of the growth to a disfavored adsorption of the metallic precursor at the NP surface due to the replacement of water molecules by ammonia in the silver ion coordination sphere.

Figure 4a shows the spectra for NPs prepared in silver ammonia solutions with different content of TMA(OH). No remarkable differences in the dipole SPR peak wavelength (415−424 nm) can be appreciated indicating that similar size and shape distributions of small, nearly spherical NPs are produced. A significant change on the tail of the SPR spectra is observed as the TMA(OH) content is raised. As stated in the previous section, for single-peak spectra, the comparison of the peak tail provides a qualitative indication of the relative abundance of large spheres and nonspherical shapes as compared

with small, nearly spherical particles. Therefore, this effect implies that increasing the concentration of TMA(OH) yields a decreasing amount of large and nonspherical NPs. It is important to mention that the overall extinction intensity of the peak (0.17–0.18) observed in the absence and in the presence of 100 μM TMA(OH) (not noticeable in the normalized plot) increases almost 60% (up to 0.28) for 1000 μM TMA(OH). This fact indicates an increase in the number of small, nearly spherical NPs. A decrease in the reaction time from 4 to 2 months and, finally, to 1 week is also observed with the increase of the TMA(OH) content. Both facts would point to an increase in the TMA(OH) concentration as a factor that favors nucleation over growth. However, it is worth noting that 100 μM TMA(OH) contributes little to favor such a trend when the metallic precursor agent is the aqueous solvated silver ion, since drastic differences were observed between the different mixing protocols (Figure 1a). Therefore, improvement of the size and shape control by favoring nucleation over growth should be mainly connected with the nature of the metallic precursor agent $[Ag(NH_3)_2]^+$, while the TMA(OH) content should contribute to a minor degree. Because TMA(OH) behaves as a strong base, it raises the pH above 9.5, increasing the OH^- concentration, which should favor the increase of the reaction rate as well as a better stabilization of the NPs. The spectra of the NPs prepared by protocols **P1** and **P2** combining the effect of using the $[Ag(NH_3)_2]^+$ as the metallic precursor and in the presence of 1000 μM TMA(OH) are shown in Figure 4b. At the end of the reaction, remarkably similar SPR profiles are obtained for both mixing protocols. The dipole SPR peak, characteristic of small, nearly spherical NPs, is defined at the same wavelength value (414 nm). Small differences are observed in the peak tail, indicating the existence of a slight difference in the size and shape distribution of the fraction of large NPs. The difference in the peak tail is directly associated with differences in the H_2Q concentration in the early stages of the reaction after the mixing of reactants since different SPR profiles were detected immediately after mixing (not shown), indicating a quick nucleation and growth of NPs in both cases. Despite that, both profiles become alike as the reaction time elapses. The continuous increase of the dipole peak extinction at 414 nm leads, in both cases, to single-peak spectra that only differ in the contribution of large NPs formed during the early stages of reaction. The growth of these large NPs is slower, while the continuous population increase of the small, nearly spherical NPs (coming from the progressive nucleation) becomes the relevant process in determining the morphology.

Figure 5a,b shows, respectively, a TEM image and the size distribution obtained from the morphological characterization of NPs grown in a silver−ammonia reactive solution containing 100 μM TMA(OH) (dashed line SPR spectrum in Figure 4a). Spheres and slightly prolate-shaped (aspect ratio from 1.2 to 2.0) particles are more frequently observed in the sample (Figure 5a), although small amounts of particles with nonregular geometry were also found. This indicates that silver−ammonia solutions allow the growth NPs with improved size control, while lesser control is achieved over the shape, which varies mainly from spheres to prolates. Considering that spheres and prolates are the main shapes, each size distribution was characterized assuming a Gaussian-type function, and the mean values are informed within the 68% confident range (Figure 5b). The average characteristic length for spheres and prolates corresponds to 14.3 ± 4.8 nm and 23.8 ± 7.6 nm, respectively, with both size distributions lying in the 5–60 nm range (Figure 5b). The average characteristic length of the NPs is considerably

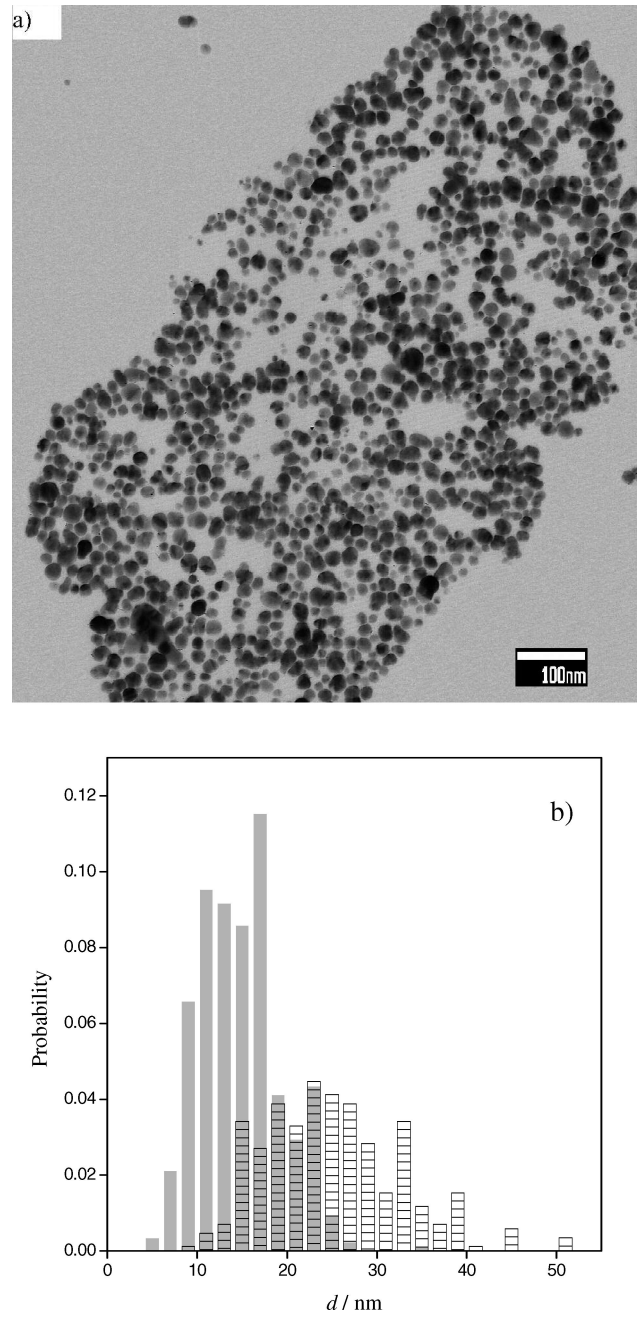

Figure 5. (a) TEM image of NPs prepared in a reactive solution also containing 1000 μM NH_3 and 100 μM TMA(OH), obtained by protocol **P2** (bar scale = 100 nm); (b) particle size distribution for spherical (full gray columns) and prolate-shaped particles (striped columns).

smaller than that observed for NPs grown in absence of ammonia (Figure 1b), in agreement with the conclusions attained for the effect of the ammonia on the basis of optical behavior.

Effect of Chloride Ions. The adsorption strength of the stabilization agent is another important factor that influences the interplay between the progressive nucleation and the NP growth. If the NP growth occurs through an autocatalytic surface mechanism,[19] the adsorption strength of the stabilization agent should play a relevant role in determining the access to surface sites for the metallic precursor and reducing agents. A better stabilization of NPs should favor nucleation over growth, as it was proposed in the previous section for the role played by the TMA(OH). At this point, it is not clear enough whether the rise in TMA(OH) content contributes to increase of the reaction

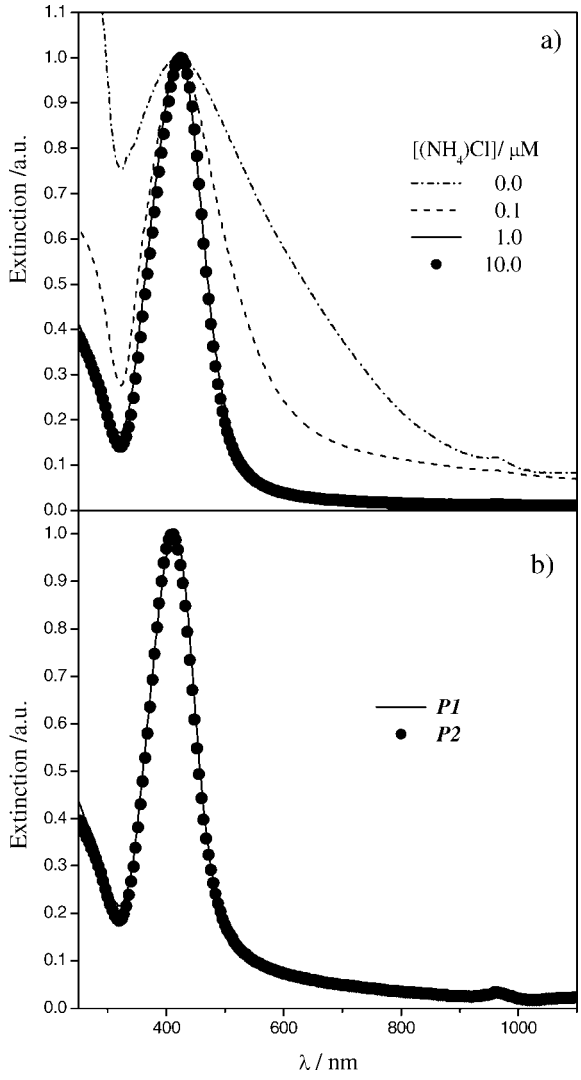

Figure 6. Normalized SPR spectra of NPs prepared in a reactive solution containing 1000 μM NH_3: (a) particles prepared by protocol **P1** for different [NH_4Cl]: (•−•) 0 μM, (−−−) 0.1 μM, (—) 1 μM, and (●) 10 μM; (b) particles preparted by different mixing protocols, (—) **P1** and (●) **P2**, to obtain a reactive solution also containing 1 μM NH_4Cl and 1000 μM TMA(OH).

rate or to favoring a better stabilization of NPs or both, since OH^- ions should be the species responsible of these effects. Therefore experiments in silver ammonia solutions were also performed in presence of different stabilization agents, namely, citrate, acetate, sulfate, and chloride anions. However, the experiments performed with chloride anions proved to be the most effective in NP stabilization. This is in accordance with the general rule that establishes that the more stable is the complex (or the salt) that a given anion forms with the silver ion the stronger is anion adsorption bonding to the surface of NPs.[22] It is worth mentioning that specific adsorption of the halides on silver metallic surfaces is a well-documented phenomenon.[23] Figure 6a shows the spectra of NPs grown in silver ammonia solutions with different content of chloride anions. The SPR peak characteristic of small nearly spherical NPs shows a very slight variation of the wavelength value (422–425 nm) for the conditions investigated, and no improvement of the stabilization can be deduced with the rise in the chloride anion content. The tail is less pronounced as the concentration of chloride anions is increased; then the fraction of large NPs diminishes. The increase in chloride content produces similar results to those already observed for increasing TMA(OH) concentration (Figure 3a); however this effect on the SPR spectra takes place within a remarkably smaller chloride concentration range. This critical range for chloride concentration can be estimated as ranging from 0.1 to 1 μM, since no significant differences can be appreciated upon increasing the concentration of Cl^- from 1 to 10 μM. The stabilization of NPs is greatly improved by chloride anions, in fair agreement with a specific adsorption of Cl^- stronger than that of OH^-. Reaction time without Cl^- (4 months) is reduced to 2 months for chloride concentration around 0.1 μM and, finally, to 20 days for chloride concentrations in the range of 1−10 μM, at the same pH value (9.5). The combined effect of TMA(OH) and NH_4Cl was also investigated and some results obtained by protocols **P1** and **P2** are shown in Figure 6b. No appreciable differences can be observed between the SPR profiles obtained with protocols **P1** and **P2**, an indication of the very small influence of the mixing protocols on the NPs formed. All the features of the SPR profile, namely, wavelength value of the dipole SPR peak (412–414 nm), peak width, and tail, are almost the same. Therefore, a better shape and size control is achieved under these conditions. Such a conclusion is supported by the morphological characterization. Figure 7 shows a TEM image of a field representative of a sample of NPs produced in these conditions, as well as their size distribution. Arranged over a large area, the NPs exhibit remarkable size and shape homogeneity (Figure 7a). The NP sizes exhibit a very narrow size distribution (Figure 7b), in the range from 5 to 25 nm, with an average characteristic length of $d = 12.4 \pm 2.8$ nm.

Despite the similarity of the final NPs produced, it is important to mention that protocols **P1** and **P2** lead to different shape and size distribution of NPs exhibiting different SPR profiles immediately after the mixing, caused by the difference in the H_2Q concentration (Figure SA2 in Supporting Information). The differences during the early stages of the reaction become less pronounced as the time elapses, and at the end of the reaction, both profiles become almost identical. Once again, this result can be explained in terms of the quenching of growth and of the increment of the population of small spherical NPs produced by the progressive nucleation.

A comment on the effect of the reducing agent concentration must be made here. At first glance, it would seem that a better control over the nucleation stage could be obtained with the rise in the H_2Q concentration. This is partially so, since it also depends on the chemical nature of the metallic precursor agent. For solutions containing the aqueous silver ion, the increase in H_2Q content makes the morphological difference of the NPs produced with protocols **P1** and **P2** diminish, yielding mainly small, nearly spherical NPs in both cases; however uncontrolled growth of large NPs is also observed (Figure SB1 in Supporting Information). As the hydroquinone concentration increases, the use of protocol **P2** leads to products with relatively lower content of large NPs, generated during the early and the further stages of reaction. This uncontrolled growth cannot be suppressed even in the presence of ammonia, where again the increase of H_2Q concentration produces an appreciable amount of large NPs (Figures SB2 and SB3 in Supporting Information).

Conclusions

We have demonstrated that the reaction of silver(I) as metallic precursor and hydroquinone as reducing agent constitutes a simple and adequate experimental model system to investigate the influence of synthetic variables on shape and size control of silver NPs. We have shown that the final NP morphology

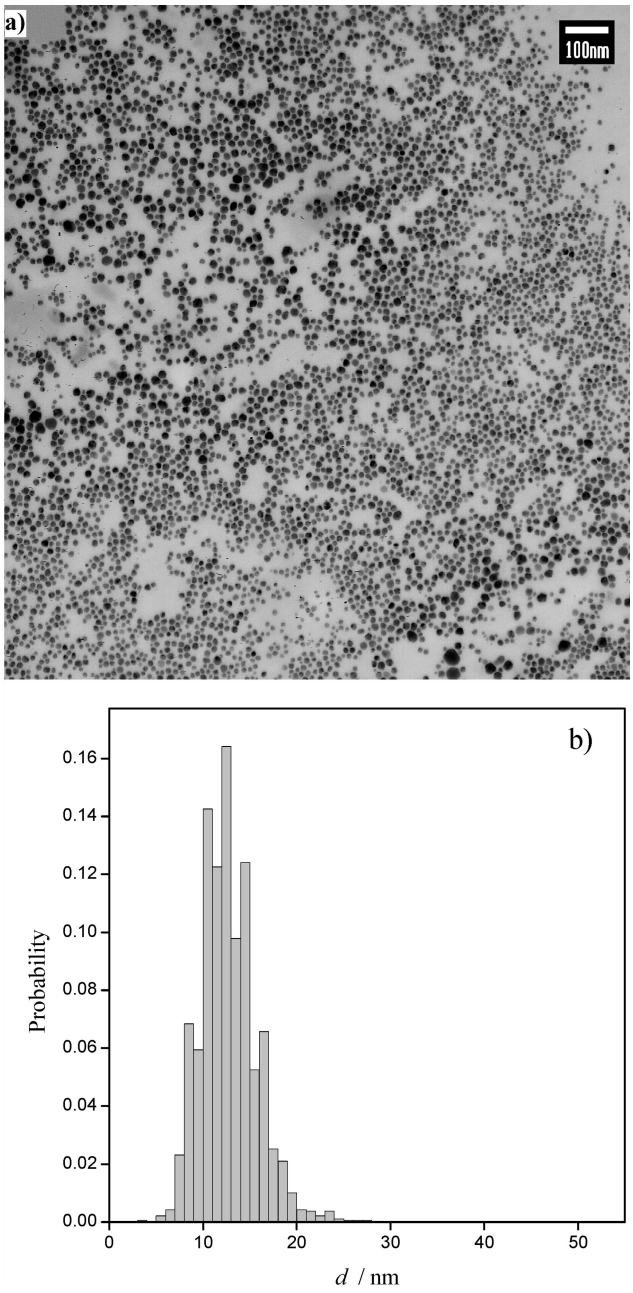

Figure 7. (a) TEM image of NPs prepared in a reactive solution also containing 1000 μM NH_3, 1 μM NH_4Cl, and 1000 μM TMA(OH) obtained by protocol **P1** (bar scale = 100 nm); (b) size distributions for Cl^--stabilized NPs.

can be strongly dependent on the local reactant concentration during the mixing process. The early stages of the reaction that take place immediately after the mixing of the reactants can determine the final morphology of NPs and, in turn, their optical properties. The evolution as well as the final NP morphology can be explained by the interplay between a progressive nucleation and an autocatalytic surface growth. The effect of the different mixing protocols on the morphology is strongly connected to the chemical nature of the metallic precursor agent. The complexation of the silver ion with ammonia leads to conditions under which the effect of the mixing protocol can be minimized, by quenching NP growth. This quenching is remarkably favored by the presence of anions that show strong specific adsorption such as chloride anions. If the reaction is driven by using the ammoniacal silver ion in presence of chloride ions, NPs synthesized exhibit a narrow size distribution due to both growth quenching and specific adsorption. Identical final optical properties of NPs obtained with different conditions of reactant mixing is a remarkable feature, which indicates that we were able to strongly minimize the influence of the early stages of the reaction on the final morphology. This in turn enables a high degree of reproducibility for the one-pot scheme in the synthesis of Ag NPs.

Acknowledgment. We thank Claudia Nome for her technical assistance in TEM. This research has been supported by the Consejo Nacional de Investigaciones Científicas y Técnicas of Argentina, the Agencia Córdoba Ciencia S.E., the Agencia Nacional de Promoción de Ciencia y Tecnología (ANPCyT), and the Secretaría de Ciencia y Tecnología (SECYT- UNC).

Supporting Information Available: Figures showing the evolution of the SPR spectra of NPs prepared under different mixing conditions with the increase of the reaction time, the effects of increase of the H_2Q concentration, and the effects of ammonia and chloride. This material is available free of charge via the Internet at http://pubs.acs.org.

References

(1) Ozin, G. A., Arsenault, A. C. *Nanochemistry: A Chemical Approach to Nanomaterials*; RSC Publishing: Cambridge, U.K., 2005.
(2) Nie, S.; Emory, S. R. *Science* **1997**, *275*, 1102.
(3) (a) Barnes, W. L.; Dereux, A.; Ebbesen, T. W *Nature* **2003**, *424*, 824. (b) Eutis, S.; El-Sayed, M. A. *Chem. Soc. Rev.* **2006**, *35*, 209. (c) Rosi, N. L.; Mirkin, C. A. *Chem. Rev.* **2005**, *105*, 1547. (d) Genet, C.; Ebbesen, W. *Nature* **2007**, *445*, 39.
(4) Mello Donegá, C.; Liljeroth, P.; Vanmaekelbergh, D. *Small* **2005**, *1*, 1152.
(5) Nikoobakht, B.; El-Sayed, M. A. *Chem. Mater.* **2003**, *15*, 1957.
(6) Jana, N. R.; Gearheart, L.; Murphy, C. J *J. Phys. Chem. B* **2001**, *105*, 4065.
(7) Liu, M.; Guyot-Sionnest, P. *J. Phys. Chem. B* **2005**, *109*, 22192.
(8) Murphy, C. J.; Gole, A. M.; Hunyadi, S. E.; Orendorff, C. J. *Inorg. Chem.* **2006**, *45*, 7544.
(9) Nikoobakht, B.; El-Sayed, M. A. *Langmuir* **2001**, *17*, 6368.
(10) (a) Jiang, X. C.; Brioude, A.; Pileni, M. P. *Colloids Surf., A* **2006**, *277*, 201. (b) Jiang, X. C.; Pileni, M. P. *Colloids Surf., A* **2007**, *295*, 228.
(11) Ha, T. H.; Koo, H.-J.; Chung, B. H. *J. Phys. Chem. C* **2007**, *111*, 1123.
(12) Pillai, Z. S.; Kamat, P. V. *J. Phys. Chem. B* **2004**, *108*, 945.
(13) (a) Murphy, C. J.; Jana, N. R. *Adv. Mater.* **2002**, *14*, 80. (b) Jana, N. R.; Gearheart, L.; Murphy, C. J. *Chem. Commun.* **2001**, 617.
(14) (a) Chen, S.; Fan, Z.; Carroll, D. L. *J. Phys. Chem. B* **2002**, *106*, 10777. (b) Chen, S.; Carroll, D. L. *Nano Lett.* **2002**, *2*, 1003.
(15) Chen, S.; Carroll, D. L. *J. Phys. Chem. B* **2004**, *108*, 5500.
(16) Henglein, A.; Giersig, M. *J. Phys. Chem. B.* **1999**, *103*, 9533.
(17) (a) Yi, H.-B.; Diefenbach, M.; Choi, Y. C.; Lee, E. C.; Lee, H. M.; Hong, B. H.; Kim, K. S. *Chem.—Eur. J.* **2006**, *12*, 4885. (b) Uchimiya, M.; Stone, A. T. *Geochim. Cosmochim. Acta* **2006**, *70*, 1388.
(18) (a) Bohren, C. F.; Huffman, D. R. *Absorption and Scattering of Light by Small Particles*; Wiley Interscience: New York, 1983. (b) Kelly, K. L.; Coronado, E.; Zhao, L. L.; Schatz, G. C. *J. Phys. Chem. B* **2003**, *107*, 668.
(19) (a) Watzky, M. A.; Finke, R. G. *J. Am. Chem. Soc.* **1997**, *119*, 10382. (b) Watzky, M. A.; Finke, R. G. *Chem. Mater.* **1997**, *9*, 3083. (c) Finke, R. G. In *Metal Nanoparticles- Synthesis, Characterization and Applications*; Feldheim, D. L., Foss, C. A., Eds.; Marcel Dekker Inc.: New York, 2002. (d) Finney, E. E.; Finke, R. G. *J. Colloid Interface Sci.* **2008**, *317*, 351.
(20) Bonnemann, H.; Nagabhushana, K. S. *J. New Mater. Electrochem. Syst.* **2004**, *7*, 93.
(21) (a) Evanoff, D. D.; Chumanov, G. *J. Phys. Chem. B* **2004**, *108*, 13948. (b) Kumbhar, A. S.; Kinnan, M. K.; Chumanov, G. *J. Am. Chem. Soc.* **2005**, *127*, 12444. (c) Malynych, S.; Chumanov, G. *J. Quant. Spectrosc. Radiat. Transfer* **2007**, *106*, 297.
(22) Henglein, A. *J. Phys. Chem.* **1993**, *97*, 5457.
(23) Magnussen, O. M. *Chem. Rev.* **2002**, *102*, 679.

CG7009644

SUPPORTING INFORMATION

Hidroquinone Synthesis of Silver Nanoparticles:A simple Model Reaction to Understand the Factors which Determine Their Growth and Nucleation.

M. A. Pérez, R. Moiraghi, E. A. Coronado and V. A. Macagno*

INFIQC – Departamento de Fisicoquímica, Facultad de Ciencias Químicas, Universidad Nacional de Córdoba, Ciudad Universitaria. 5000 Córdoba, Argentina.

E-mail address: mperez@fcq.unc.edu.ar (M. A. Pérez)

A- The Early Stages of the Reaction with Different Mixing Protocols

1) 100 µM $AgNO_3$ + 5 µM H_2Q + 100 µM TMA(OH)

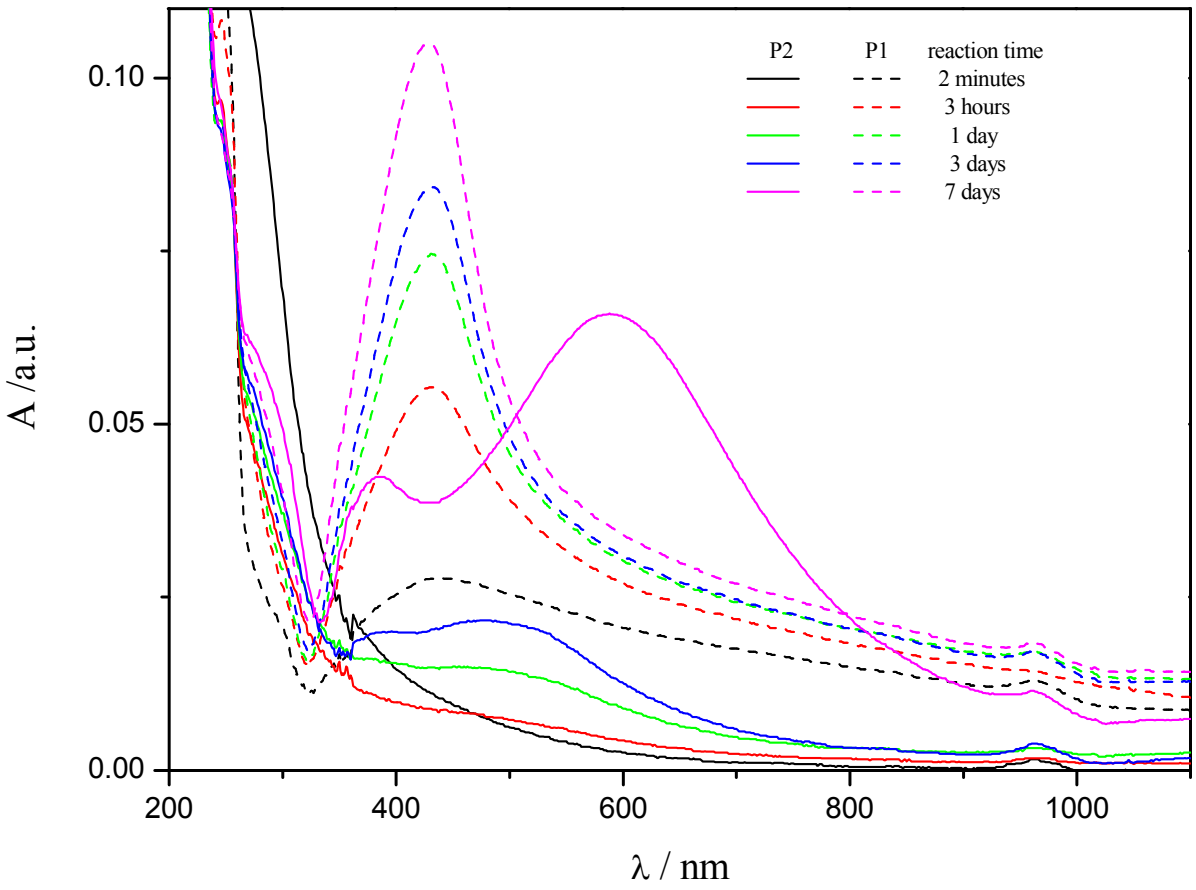

SA1. Evolution of the SPR's spectra of NP's prepared with ***P1*** (dashed lines) and ***P2*** (solid lines) for reaction time of: (black) 2 minutes immediately after the mixing of reactants, (red) 3 hours, (green) 1 day, (blue) 3 days, and (magenta) 7 days.

The spectra exhibit noticeable differences in their shapes, indicating that the NP's obtained under different mixing conditions present drastic differences in their size/shape distribution. Immediately after the mixing of reactants, ***P1*** leads to a spectrum with a peak around 435 nm and a long tail extended within the whole visible range. On the contrary, for ***P2*** the characteristic dipole SPR of small spheres is absent. As the reaction time elapses, the SPR peak of NP's prepared with ***P1*** increases continuously with no remarkable changes in the shape of the profile, indicating that the increase of the number of small spherical NP's generated by progressive nucleation constitutes the main process. In the case of the NP's obtained with ***P2***, the SPR profile evolves to define a doubly-peaked spectrum. The peak at longer wavelength values red-shifts with the development of the reaction, indicating that NP's become larger.

2) 100 μM $AgNO_3$ + 5 μM H_2Q + 1000 μM NH_3 + 1000 μM TMA(OH)

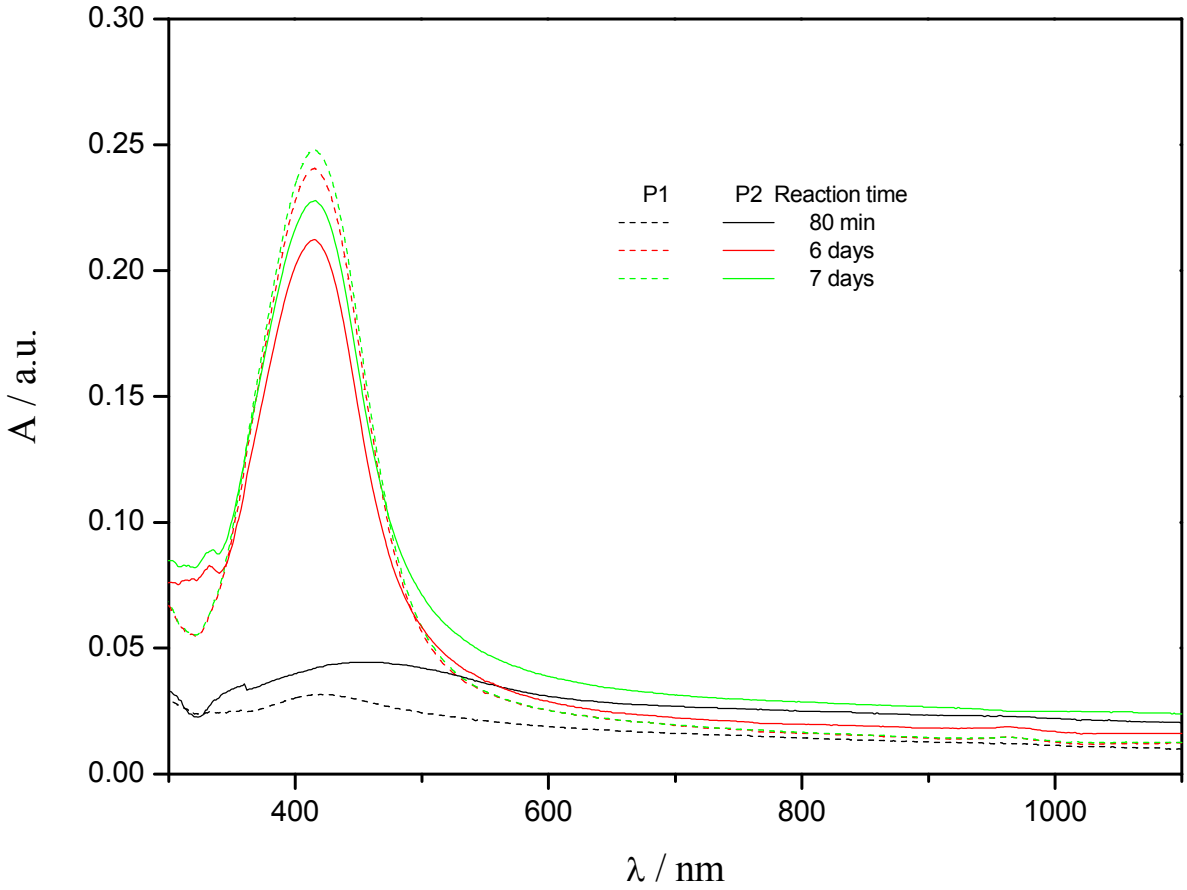

SA2. Evolution of the SPR's spectra of NP's prepared with ***P1*** (dashed lines) and ***P2*** (solid lines) for reaction time of: (black) 80 minutes immediately after the mixing of reactants, (red) 6 days, (green) 7 days.

Different mixing conditions lead during the early stages of the reaction to different spectra, however as the reaction time elapses the SPR profiles become similar. The uncontrolled events during the mixing that generate different shape/size distribution have a minor influence on the final morphology of the NP's. The continuous increase observed in the SPR peak at 414 nm is associated with the increment of the amount of small spherical NP's coming from the progressive nucleation.

B- Increase of the H_2Q Concentration

1) 100 μM $AgNO_3$ + 100 μM TMA(OH), *P2*

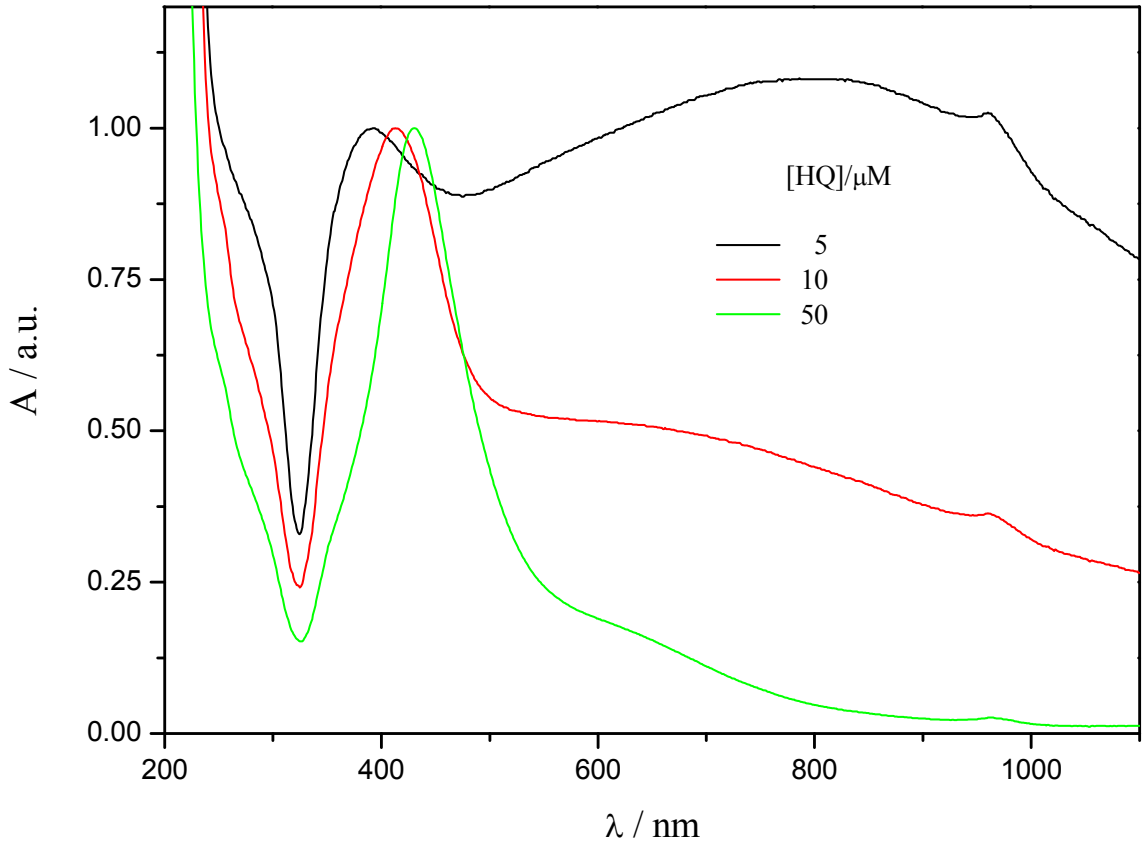

SB1. Normalized SPR's spectra of NP's prepared with ***P2*** for increasing H_2Q concentration.

The increase of H_2Q concentration leads to rise of the number of small spherical NP's which is evidenced by the red shift observed for the series of spectra around 400 nm. The characteristic dipole SPR maximum of large NP's (800 nm) also decreases becoming an ill defined peak and, finally, a shoulder of the main SPR peak at around 400 nm. Under the present conditions, the increase of H_2Q produces a large amount of small spherical NP's, however some large NP's coming from an uncontrolled growth are also obtained.

2) 100 μM $AgNO_3$ + 1 μM NH_4Cl + 1000 μM NH_3, *P2*

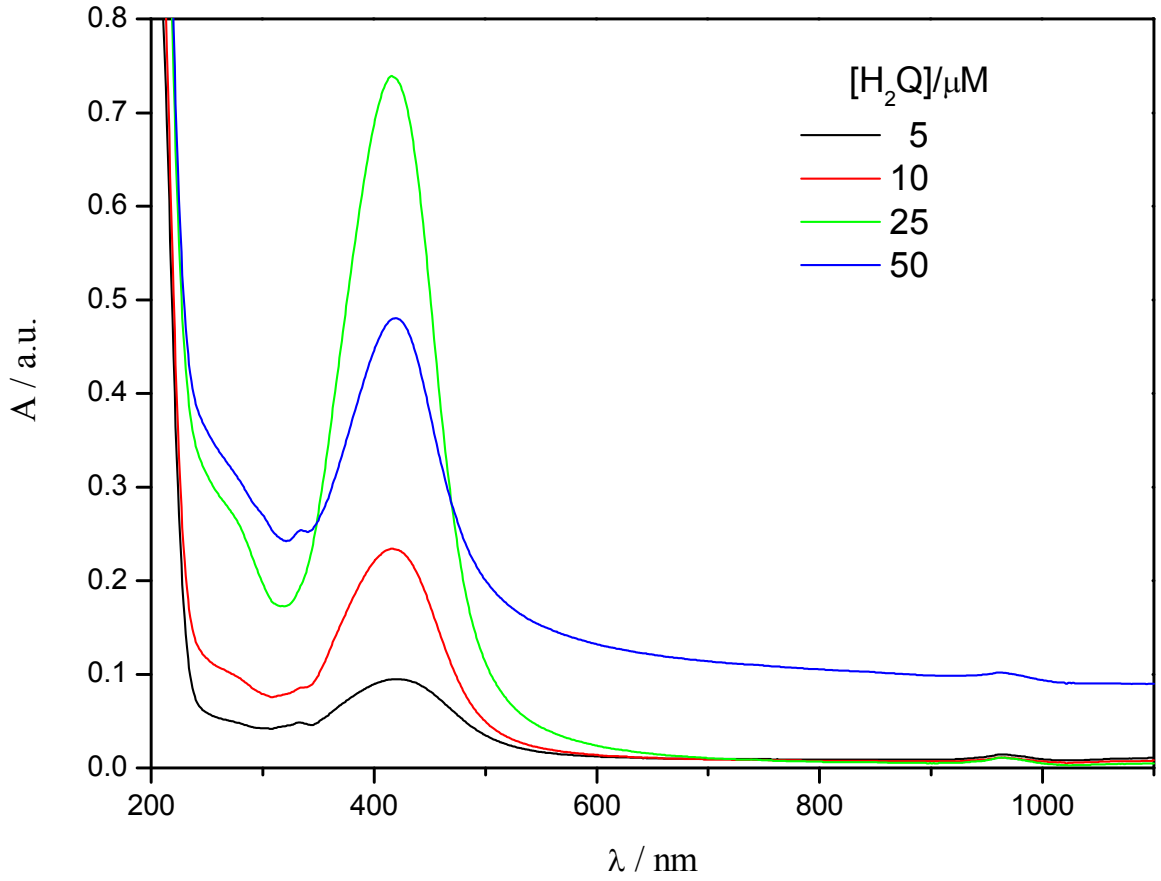

SB2. SPR's spectra of NP's prepared with ***P2*** for increasing H_2Q concentration.

The rise of the number of small spherical NP's caused by the increase of H_2Q concentration is observed as an increase of the peak at around 400 nm, however a noticeable tail is observed for the highest concentration value. This last feature is a clear indication that the increase of H_2Q concentration does not always favour the formation of small spherical NP's, even for conditions under which the growth is quenched.

3) 100 μM $AgNO_3$ + 50 μM H_2Q + 1 μM NH_4Cl + 1000 μM NH_3, *P2*

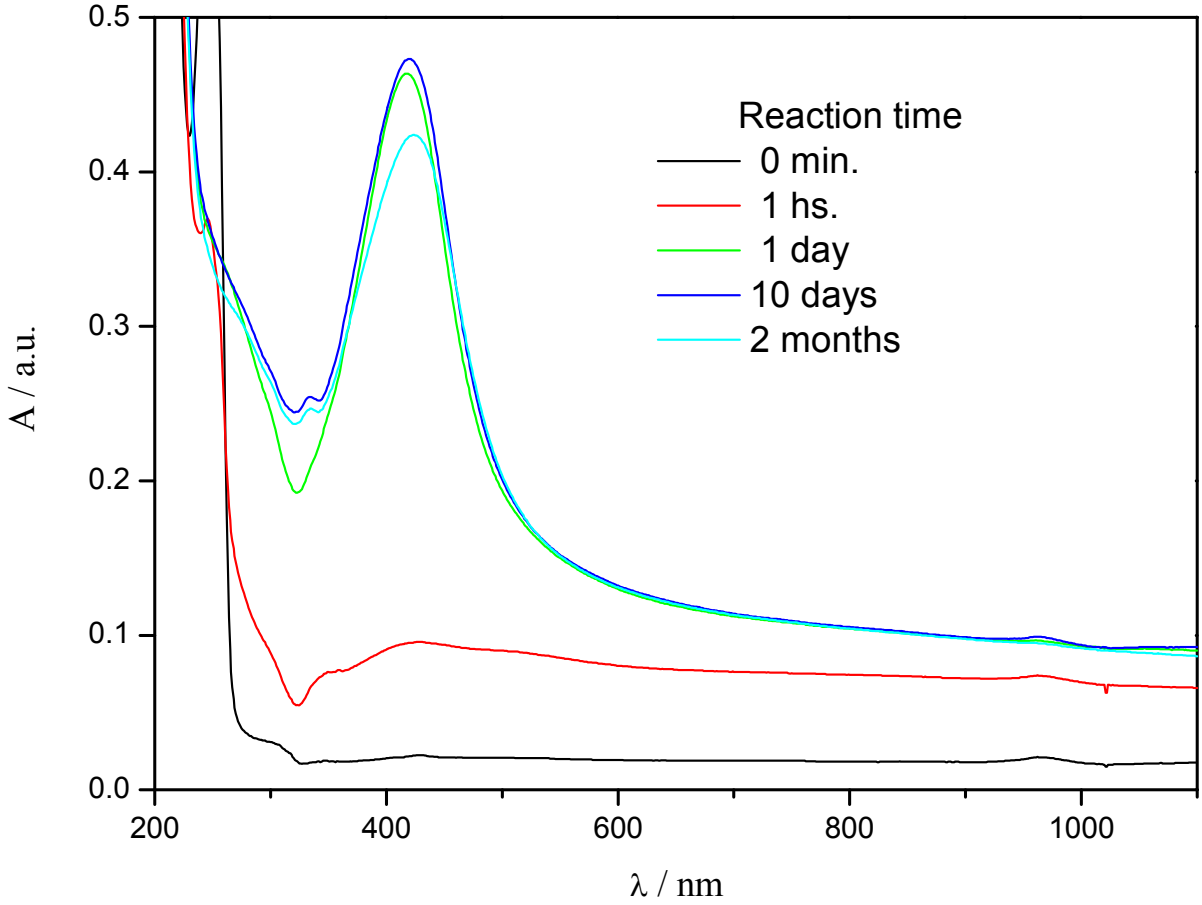

SB3. Evolution with the reaction time of the SPR's spectra of NP's prepared with ***P2*** for 100 μM $AgNO_3$ + 50 μM H_2Q + 1 μM NH_4Cl + 1000 μM NH_3.

The changes of the SPR profile during the reaction indicates that NP's morphology is determined by a complex interplay between progressive nucleation and autocatalytic surface growth. At high concentration of H_2Q (50 mM), an uncontrolled growth is observed during the early stages of the reaction, as is evidenced by the SPR profiles extended in the whole visible range. The quenching effect of silver ammonia complex on the catalytic surface growth is limited under these conditions. As the reaction time elapses, the decrease of H_2Q concentration makes the quenching of the autocatalytic surface growth more important, leading again to an increase of the amount of small spherical NP's (evidenced by the SPR peak at around 400 nm).